

Metal-organic Frameworks at the Bio-interface: Synthetic Strategies and Applications.

Christian Doonan^{1,}, Raffaele Riccò², Kang Liang³, Darren Bradshaw^{4,*}, and Paolo Falcaro^{1,2,*}.*

1. School of Physical Sciences, The University of Adelaide, Adelaide, South Australia 5005, Australia.

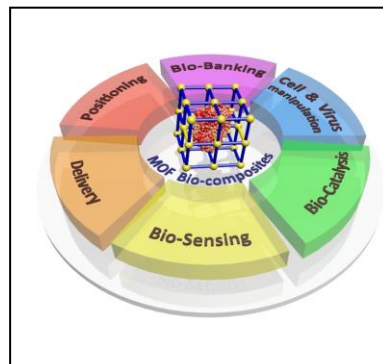
2. Institute of Physical and Theoretical Chemistry, Graz University of Technology, Stremayrgasse 9, Graz 8010, Austria.

3. CSIRO Private Bag 10, Clayton South, Victoria 3169 Australia.

4. School of Chemistry, University of Southampton, Highfield Campus, Southampton SO17 1BJ, UK.

Conspectus

Many living organisms are capable of producing inorganic materials of precisely controlled structure and morphology. This ubiquitous process is termed biomineralization and is observed in nature from the macroscopic, e.g. formation of exoskeletons, down to the nanoscale, e.g. mineral storage and transportation in proteins. Extensive research efforts have pursued replicating this chemistry with the overarching aims of synthesizing new materials of unprecedented physical properties and understanding the complex mechanisms that occur at the biological-Inorganic interface.



Recently, we demonstrated that a class of porous materials termed Metal-organic Frameworks (MOFs) can spontaneously form on protein-based hydrogels via a process analogous to natural matrix-mediated biomineralization. Subsequently, this strategy was extended to functional biomacromolecules, including proteins and DNA, which have been shown to seed and accelerate crystallization of MOFs. Alternative strategies exploit co-precipitating agents such as polymers to induce MOF particle formation thus facilitating protein encapsulation within the porous crystals. In these examples the rigid molecular architecture of the MOF was found to form a protective coating around the biomacromolecule offering improved stability to external environments that would normally lead to its degradation. In this way, the MOF shell mimics the protective function of a biomineralized exoskeleton. Other methodologies have also been explored to encapsulate enzymes within MOF structures, including the fabrication of polycrystalline hollow MOF micro-capsules that preserve the original enzyme functionality over several batch reaction cycles. The potential to design MOFs of varied pore size and chemical functionality has underpinned studies describing the post-synthesis infiltration of enzymes into MOF pore networks and bioconjugation strategies for the decoration of the MOF outer surface, respectively. These methods and configurations allow for customized biocomposites.

MOF biocomposites have been extended from simple proteins to complex biological systems including viruses, living yeast cells and bacteria. Indeed, a noteworthy result was that cells encapsulated within a crystalline MOF shell remain viable after exposure to a medium containing lytic enzymes. Furthermore, the cells can adsorb nutrients (glucose) through the MOF shell but cease reproducing until the MOF casing is removed, at which point normal cellular activity is fully restored.

The field of MOF biocomposites is expansive and rapidly developing towards different applied research fields including protection and delivery of biopharmaceuticals, bio-sensing, bio-catalysis, bio-banking, cell and virus manipulation. This account will describe the current progress of MOFs towards biotechnological applications highlighting the different strategies for the preparation of biocomposites, the developmental milestones, the challenges and the potential impact of MOFs to the field.

1. Introduction

Research on metal-organic frameworks (MOFs) has rapidly progressed from studying aspects of their fundamental chemistry¹ to pursuing applications in the multidisciplinary areas of nanotechnology and materials science.^{2,3} MOFs are synthesized via a ‘building block’ approach from organic linkers and metal nodes, offering control of chemical functionality, pore shape and size and crystal morphology.⁴ These mutable properties have facilitated their application in biologically related fields.⁵ For example, MOFs with large internal pore volumes and tunable crystal size have been employed in drug delivery studies,⁶ including preliminary *in vivo* investigations.⁷ Furthermore, inspired by natural biomineralization, we have demonstrated how biomacromolecules,⁸ biomaterials,⁹ and cells¹⁰ can efficiently promote MOF crystallization establishing the important first steps toward MOF-based biomaterials that may be of practical use in industrial biocatalysis and biobanking. An important conclusion derived from these studies is that the development of this area requires a fundamental understanding of MOF formation at bio-interfaces.¹¹

MOF biocomposites can be categorized according to how their (biological) components are integrated, namely via bio-conjugation, infiltration, or encapsulation (Scheme 1). Bio-conjugation is defined as the *adsorption or covalent attachment* of a biomacromolecule on the outer surface of MOF crystals (Scheme 1b). The second class are generated by *infiltrating* biomolecules into the pore networks of MOFs (Scheme 1c) through non-covalent interactions: since the pore size of the MOF is must be larger than the biomacromolecule, generally limiting the approach to mesoporous MOFs. The third biocomposite type is formed by assembling the MOF under biologically compatible reaction conditions in a medium containing

biomacromolecules, leading to their *encapsulation* within the MOF architecture (Scheme 1d) while preserving the biomolecules intrinsic functionality.

In this account we canvass the initial discoveries and progress of MOF biocomposites, highlighting each of the synthetic strategies and identifying the future challenges in this emergent field of research.

2. Surface bio-conjugation.

Two general approaches have been employed for anchoring biomacromolecules to the external surface of MOF particles: 1) *grafting*, whereby the biomacromolecule is covalently attached to the MOF (Figure 1a-b) and, 2) *adsorption*, whereby the biomacromolecule is adhered to the surface of the MOF via non-covalent interactions (*e.g.* hydrogen bonding, van der Waals or electrostatic attraction Figure 1c-e). We note that surface functionalization can also engender *partial infiltration* of the biomacromolecule into the MOF pore network.

2.1 Grafting.

The organic components of MOFs can provide moieties such as carboxylic acid and amino groups that can act as anchoring points for biomacromolecules.^{12–14} In 2012 Huang, Lin, and coworkers covalently bound biomacromolecules to MOFs (**Table 1**)¹² using a DCC-mediated coupling reaction between protein –NH₂ and MOF-based –COOH groups, where trypsin (EC 3.4.21.4) could be grafted onto MIL-88B-NH₂(Cr) to afford a reusable BSA digestion system. Although the amino moiety of MIL-88B-NH₂(Cr) was not directly involved in the coupling reaction, it enhanced trypsin immobilization (and BSA digestion) via hydrogen bonding interactions. In 2015, Lei and coworkers employed the classical two-step EDC/NHS method¹⁵ to graft streptavidin to the free –COOH groups of a MOF-based composite consisting of HKUST-1

and FeTCPP.¹³ This novel HKUST-1-FeTCPP-streptavidin biocomposite was subsequently used as an electrochemical DNA sensor. MOF biocomposites have also been synthesized using homobifunctional glutaraldehyde, a common protein crosslinking agent.¹⁶ For example, in 2013, Falcaro and coworkers used glutaraldehyde to immobilize β -glucosidase (EC 3.2.1.21) onto patterned films of NH₂-MIL53(Al) (Figure 1b)¹⁷. Similarly, Lou and coworkers grafted SEH hydrolase (EC 3.3.2.9) onto NH₂-UiO66; the resulting biocomposite was used to prepare enantiopure vicinal diols by stereospecific epoxide ring opening of 1,2-epoxyoctane in water.¹⁸

Grafting biomacromolecules to the surface of MOFs requires specific functionalization that may not be compatible with all MOFs. Furthermore, this strategy does not take advantage of the large pore volumes typical of MOF materials.

2.2 Adsorption.

Surface functionalization via adsorption relies on non-covalent interactions, such as electrostatic attraction between the positively charged metal clusters of MOFs and negatively charged regions of proteins rich in Glu and Asp residues or hydrogen bonding interactions that can occur between free carboxylic, amino, or imidazole-based MOF ligands and biomacromolecules (**Table 2**). Another non-covalent approach to surface functionalization involves partial infiltration of the biomacromolecule within the MOF pore network: *e.g.* Huang and Lin^{19–21} immobilized Trypsin onto various MOFs by tagging the enzyme with NBD.²⁰ The NBD facilitates a strong host–guest interaction arising from a close match between the molecular dimensions of the dye and pore window of the MOF. This ‘finger-insertion’ strategy also stabilizes the immobilized enzyme through multipoint attachment.²¹

In general, surface functionalization does not require a MOF with pores larger than the biomacromolecule (Scheme 1b), therefore microporous MOFs (pores \leq 2 nm) including MILs,

HKUST-1 and UiO-66 have been employed. However, in the case of “finger-insertion”, the MOF pores should match the dimensions of the guest to maximize host–guest interactions.²⁰

3. Infiltration into MOFs.

The pore networks of MOFs are known to host a wide variety of guests ranging from gas molecules to nanoparticles.² Incorporating biomacromolecules within MOFs presents a challenge however as their size typically exceeds micropore dimensions (Figure 2), thus large pore MOFs (*e.g* MIL100; NU-100x class; porous coordination networks (PCNs); IRMOF-74 series) are required. Ma’s group first demonstrated infiltration of cyt c²² myoglobin,²³ and MP-11^{24,25} into a mesoporous H₃TATB ligand-based MOF. Subsequently, Yaghi’s group synthesized isorecticular analogues of MOF-74 yielding materials with hexagonal channels up to ~10 nm in diameter that could be infiltrated with vitamin B₁₂ and GFP.²⁶ In 2016, Farha’s group demonstrated a novel application for proteins occluded within MOF architectures. Here an organophosphorus nerve agent detoxifying enzyme, OPAA, was infiltrated into MOF pores (NU-100x and PCNs) to carry out the decomposition of both nerve agents and their simulants.^{27,28} Indeed, the catalytic efficiency of the immobilized enzyme was found to be greater than the free enzyme highlighting the potential biotechnological applications for such systems. Biomacromolecules vary extensively in shape and size, thus a key challenge when adopting this strategy is that MOFs possessing compatible pore dimensions need to be identified on a case-by-case basis, and may require bespoke frameworks giving rise to a further level of complexity for different applications (Table 3).

4. Encapsulation strategies

Encapsulation of functional biomolecules in hollow spherical MOF architectures represents a novel strategy for synthesizing MOF biocomposites.^{29–31} This requires the MOF in a microcapsule configuration (**Figure 3**), typically obtained using templates around which a well-defined MOF shell can grow. Soft^{29,30} and hard³¹ templates can be employed, and a favored approach is MOF formation around a biomolecule-containing emulsion droplet. Pickering-stabilized hydrogels²⁹ and continuous-flow microfluidic protocols³⁰ have met with a good degree of success, allowing a range of biomolecules to be encapsulated. The main advantages of this method include the ability to incorporate enzymes far greater in size than MOF micropores, and to permit the biomolecules to operate in a dynamic environment within the capsule.

4.1 Soft Templating

Huo *et al.* employed agarose hydrogel droplets Pickering-stabilized with UiO-66 and Fe₃O₄ nanoparticles as a substrate to deposit a hierarchically-structured ZIF-8 shell (**Figure 3a-c**).²⁹ The ~40 µm diameter capsules contain both UiO-66 and magnetite particles, and the shell consists of an open network-like aggregate of ZIF-8 nanoparticles capped by a dense over-layer of inter-grown ZIF-8 crystals, which controls molecular access to the capsule interior. Biomolecules added to the hydrogel droplets could be readily incorporated into the capsules, yielding magnetic MOF-based bioreactors.²⁹ Through careful design of capsule assembly and choice of emulsion-stabilizing particles, multiple functional species (inorganic and biological) can be incorporated into a single system. Following enzyme loading, the biomolecules were found to be concentrated around the interior surface of the capsule; however, solvent-dependent enzyme mobility within the capsule was also demonstrated. An encapsulated CalB lipase was

found to be 5 times more active than the free enzyme for transesterification reactions. The microporous ZIF-8 shell permitted size-selective biocatalysis, and activity was maintained at 80% over 6 cycles.

In collaboration with Kim's group we exploited a microfluidic continuous-flow system to prepare well-defined capsules of MIL-88A (**Figure 3d-h**).³⁰ Aqueous droplets containing the metal component were injected into a 1-octanol stream containing the organic linker, and transported through a microreactor loop at 40 °C. MOF formation occurs at the droplet interface, and nearly monodisperse capsules with controllable diameter between 30-2000 μm were rapidly fabricated.³⁰ Inclusion of nanoparticles or biomolecules into the aqueous phase permits their encapsulation within the hollow MIL-88A microspheres. Enzymatic activities of encapsulated GDH, HRP and AChE were preserved over 4 cycles, and in the case of GDH the product yield exceeded that of the free enzyme by >50%. Activity of encapsulated AChE was further maintained in the presence of an inhibitor, confirming the protective role of the MOF shell. The microfluidic system can also be configured to form double-shell MOF capsules, for the possible compartmentalization of reactive species or to carry out sophisticated cascade reactions.

4.2 Hard Templating

Recently, Wang *et al.* reported a hard templating strategy for the encapsulation of GOx within a PDA/ZIF-8 capsule for glucose sensing³¹, where PDA-coated GOx-embedded CaCO_3 microspheres were used as templates to grow ZIF-8 shells. The resulting GOx@PDA/ZIF-8 capsules were covered in graphene nanosheets and immobilized onto a glassy carbon electrode to produce a glucose sensor following reaction with GOx, and the breakdown of generated H_2O_2 by ZIF-8. The resulting flow of electrons between the capsules and the electrode was facilitated by the adsorbed graphene sheets, and the amperometric response recorded.³¹ The electrochemical

biosensor displayed excellent selectivity and stable glucose detection with an estimated detection limit of 0.33 μM . This work demonstrated how MOF-encapsulated biomolecules can be integrated into functioning devices, an important future direction for this research area.

4.3. One-pot Embedding

Recent studies have shown that biomacromolecules can promote rapid growth of MOFs (Figure 4). The concept of encasing a protein within a MOF that has pores of significantly smaller dimensions than the guest was first proposed by Ge and Liu.³³ When PVP-modified cytc was added to a methanol solution of ZIF-8 precursors a crystalline precipitate of ZIF-8 rapidly formed. Pertinently, the activity of the encapsulated enzyme showed a remarkable 10-fold enhancement compared to the same concentration of free cytc in solution. Although PVP coated inorganic nanoparticles³⁴ had previously been employed as MOF nucleating agents, the encapsulation of functional biomacromolecules constitutes an important advance, and the wider applicability of this co-precipitation strategy towards different enzymes and framework materials has also been demonstrated^{32,33,35}. For example, encapsulation of PVP coated catalase within ZIF-90³² allowed the protein to retain activity in a solution containing proteinase, demonstrating that the MOF pores offer size selective access to the enzyme. It is noteworthy that alcohol was not used in biocomposite synthesis as it can have a deleterious effect on enzyme activity.³²

We have shown that neither PVP nor alcohol is necessary for MOF encapsulation of biomolecules. When amino acids, DNA and proteins (i.e. serum albumin, enzymes, and antibodies) are added to aqueous solutions of zinc acetate and 2-methylimidazole, ZIF-8 particles with biomacromolecule-dependent morphologies are rapidly formed. This water-only approach is termed ‘biomimetic mineralization’ due to its similarities to natural biomineralization

processes.⁸ The capacity of the MOF shell to protect enzymes from inhospitable environments is exemplified by a series of experiments performed on HRP@ZIF-8, where exposure to boiling water or organic solvents (e.g. N,N-dimethylformamide at 150°C) had a negligible effect on activity. Furthermore, the HRP@ZIF-8 biocomposite outperformed other commonly employed porous carriers (i.e. calcium carbonate; mesoporous silica nanoparticles) when the enzyme activity was measured under analogous conditions. The MOF's remarkable ability to protect proteins from denaturing occurs by tightly encapsulating them in cavities that are 10-30% larger than the guest dispersed within the host crystal structure as evidenced by synchrotron SAXS analysis.. Further stabilization of the protein structure was supported by FTIR studies which revealed stretching frequencies attributed to bonding interactions between the biomolecule and the framework-forming Zn cations.⁸ Encapsulated biomolecules can be released intact from the ZIF-8 network by lowering the pH from neutral to 6, indicating the pH sensitivity of ZIF-8 could be exploited for controlled biomolecule release.

We recently performed a comparison between the two different methods for biomolecule encapsulation: PVP-mediated co-precipitation and biomimetic mineralization³² using Urease as the guest. Although both methods stabilized the enzyme towards inhospitable conditions, subtle differences were observed with respect to crystal size and biomolecule distribution within the composites. Co-precipitation gave rise to crystals of average size ca. 120 nm, irrespective of the molecular weight of the PVP used, with guest cavities generally located towards the surface. However, biomimetic mineralization yielded Urease@ZIF-8 crystals ca. 500 nm in size and a homogenous distribution of guest cavities. Subsequent to our initial studies the biomineralization strategy has been employed to encapsulate thermophilic lipase in ZIF-8,³⁶ while a model antigen used in immunization research (ovalbumin) was successfully encapsulated in ZIF-8 using the co-

precipitation method; this composite was used for the controlled delivery of ovalbumin to cells.³⁷ These recent studies further confirm the potential of MOF biocomposites for bioprocessing and biopharmaceutical delivery (**Table 4**).

5. Biomimetic mineralization of MOFs from biological surfaces

Porous coatings of MOFs on biologically active surfaces are at the interface of biology and materials science and could lead to new applications in biomedical research and diagnostic devices.

A pioneering study describing how gelatin hydrogel surfaces can initiate MOF crystallization via a process analogous to natural biomineralization was carried out by Bradshaw's group.⁹ Their approach involved adding metal salts during the gelatin formation resulting in cation-embedded hydrogels. Upon the introduction of solutions containing HmIm or H₃BTC, ZIF-8 or HKUST-1 particles, respectively, formed on the gelatin fibers.

These initial studies were progressed by showing that films and patterns of proteins (e.g. BSA) could be used to localize MOF growth.³⁸ For example, exposure of MOF precursors to a protein film fabricated by drop-casting onto a silicon wafer led to the rapid formation of crystals on the protein film suggesting biomacromolecules can act as preferential MOF nucleation sites. We note that although the addition of MOF precursor solution detached some proteins from the surface (c.a. 38% loss in the case of ZIF-8), a continuous MOF film was nonetheless observed (Figure 5a-b). The scope of this work was examined by using macroscopic and microscopic protein patterns generated using contact printing³ and microfluidic-pen lithography³⁹, respectively, as MOF nucleation sites. The efficiency of this approach was demonstrated by

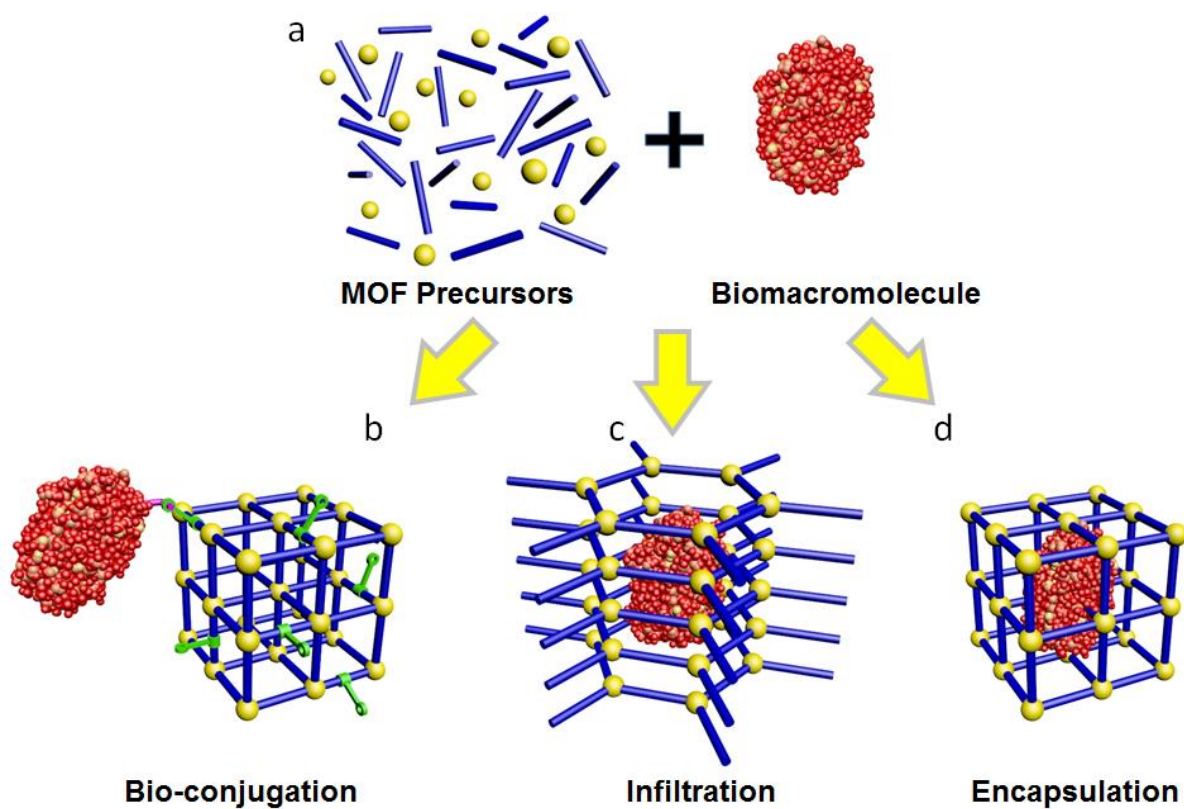
showing that luminescent MOFs, $\text{Ln}_2(\text{BDC})_3$ ($\text{Ln} = \text{Tb}, \text{Eu}, \text{Ce}$) could be formed within 30 s on protein patterns and finger print residues (Figure 5c-d).

Zhang and coworkers showed that MOFs can be grown on yeast cell surfaces⁴⁰, hypothesizing that the yeast cell walls attract metal ions and serve as a reservoir for the formation of MOF crystals. Subsequently, we demonstrated that MOFs could be used to coat and protect living yeast cells from environments that would normally promote their death.¹⁰ Introduction of ZIF-8 precursors to dispersed cells yielded a crystalline coating within 10 min (Figure 5e-g). Remarkably, the MOF shell had minimal impact on cell viability (Figure 5h) while controlling molecular trafficking to and from the cell by preventing the diffusion of antifungal drugs and cell lytic enzymes to the cells, but allowing essential nutrients (e.g. glucose) through their pore network. The MOF coating prevented cell division and upon shell removal the cells immediately regained full growth kinetics. ZIF-8 coatings were also successfully formed on bacteria (*Micrococcus Luteus*)¹⁰ further demonstrating the potential of the method for cell coating applications. Interestingly, Gassensmith's group recently established that a ZIF-8 coating with tunable thickness could be formed on Tobacco Mosaic Virus, allowing for a consequent controlled chemical modification through the permanent porosity of the framework, while preserving its original capsid shape.⁴¹

Very recent work by Naik and Singamaneni demonstrated how MOF coatings preserved the bio-recognition capabilities of surfaces based on bio-conjugated antibodies (e.g. IgG/anti-IgG) after exposure to elevated temperatures (40 and 60 °C). This clearly shows the potential of MOFs for the fabrication of antibody-based biochips with improved stability to ambient and elevated temperatures.⁴²

Future directions and Applications

Research focused on MOFs and biomacromolecules has moved towards the exploration of novel biocomposites that have already demonstrated promise in the fields of biosensing, biocatalysis, and the storage/delivery of biopharmaceuticals. Biomimetic mineralization is the most recently explored approach to the synthesis of MOF biocomposites and has many exciting possibilities for bio-based applications. The encapsulation process is rapid and preserves the biomacromolecule from external environments that would typically lead to its degradation. Accordingly, it can be envisaged that biobanking and transport of high-value, fragile, biomacromolecules without a ‘cold-chain’ are areas that could benefit from this technology in the near future whereas developing these systems for industrial biocatalysis is a longer-term prospect. However, to fully realize the potential applications and new opportunities of MOF biocomposites further fundamental research is required. For example, a precise understanding of how proteins and living cells induce the growth of MOFs and affect their structure and morphology is essential. Such knowledge will facilitate the development of general protocols for encapsulation of biomacromolecules and for crystallizing MOFs on tissues and living organisms and will underpin exploration of biomedical applications.



Scheme 1. MOF biocomposites are obtained by bio-conjugation, infiltration, or encapsulation of biomacromolecules with MOF precursors

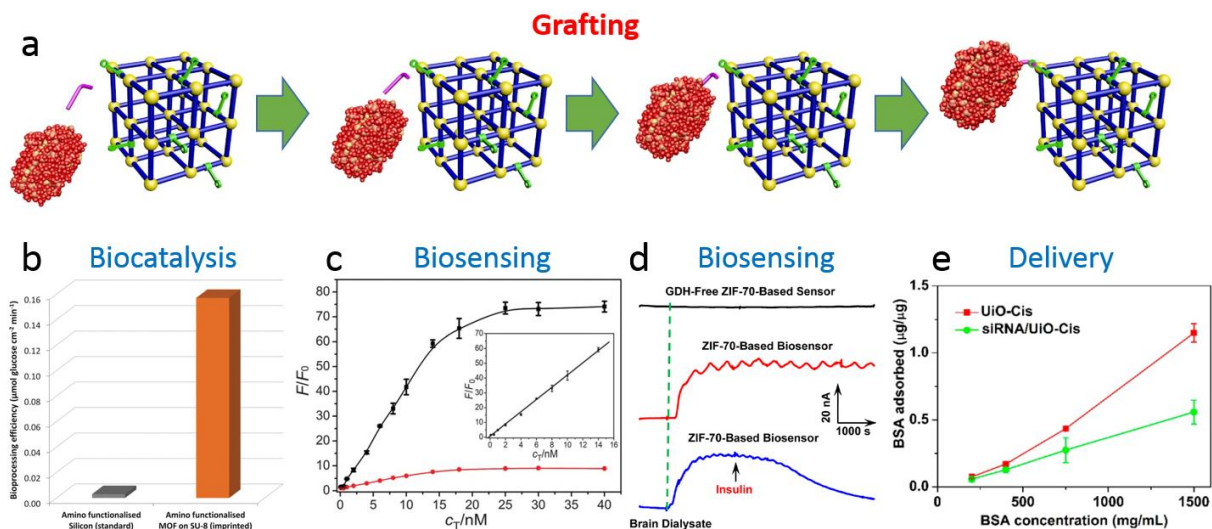


Figure 1. (a) Grafting of biomolecules on MOFs; in case of β -glucosidase grafted on NH_2 -MIL53(Al) MOF the biocomposite has enhanced biocatalytic activity (b);¹⁷ (c) Signal-to-background ratio of SYBR Green/DNA probe/MIL101 complex with increasing concentration of target DNA;⁴³ (d) Online current–time response recorded for the brain microdialysates of guinea pig with the ZIF-70 based electrode detector;⁴⁴ (e) BSA binding to UiO-Cis MOF with and without siRNA loading.⁴⁵ (Reproduced with permission from the refs.: [17]. Copyright 2013 WILEY-VCH, [43]. Copyright 2014 Royal Society of Chemistry, [44],[45]. Copyright 2013-2014 American Chemical Society)

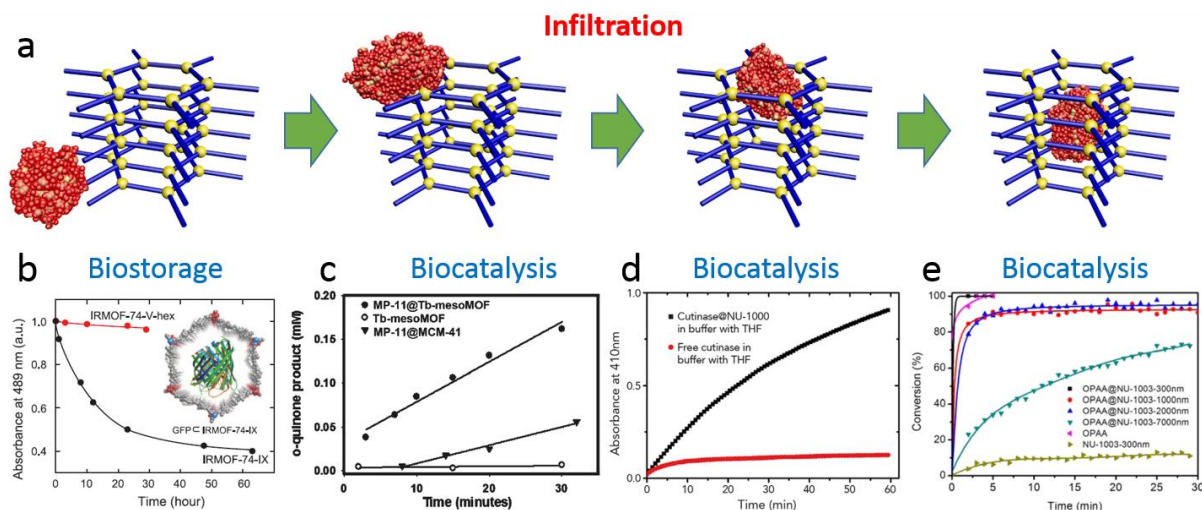


Figure 2. (a) The infiltration into MOFs is achieved when the biomacromolecule fits the pore size. (b) Inclusion study of GFP into large pore MOF-74 isorecticular MOF;²⁶ (c) kinetic study for the 3,5-di-t-butyl-catechol oxidation by MP-11@Tb-mesoMOF;²⁴ (d) reaction kinetics of p-nitrophenylbutyrate hydrolysis by Cutinase@NU-1000;⁴⁶ (e) hydrolysis profiles of diisopropyl fluorophosphate catalyzed by various OPAA@NU-1003 MOF biocomposites.²⁷ (Reproduced with permission from the refs.: [26]. Copyright 2012 Science AAAS, [24],[27]. Copyright 2011 American Chemical Society, [46]. Copyright 2016 Elsevier)

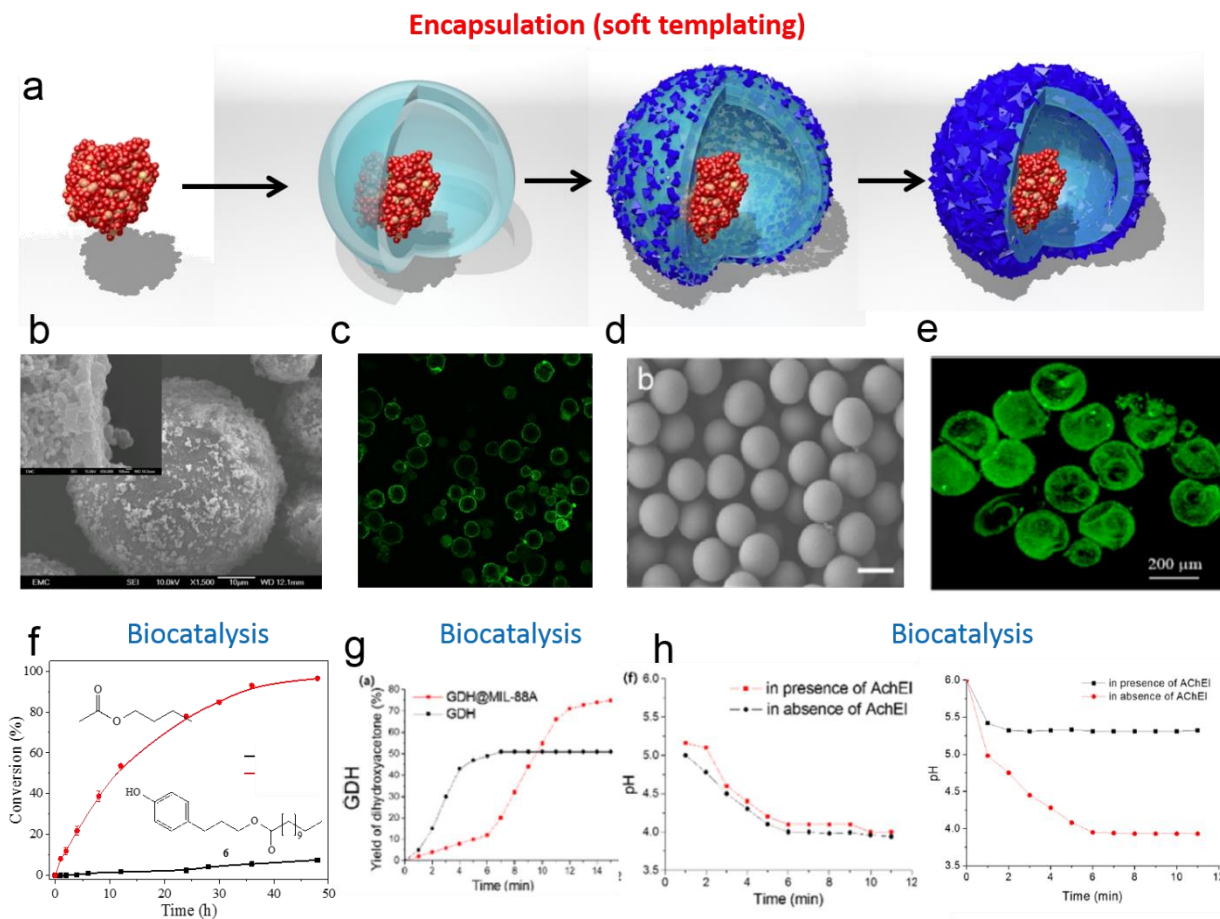
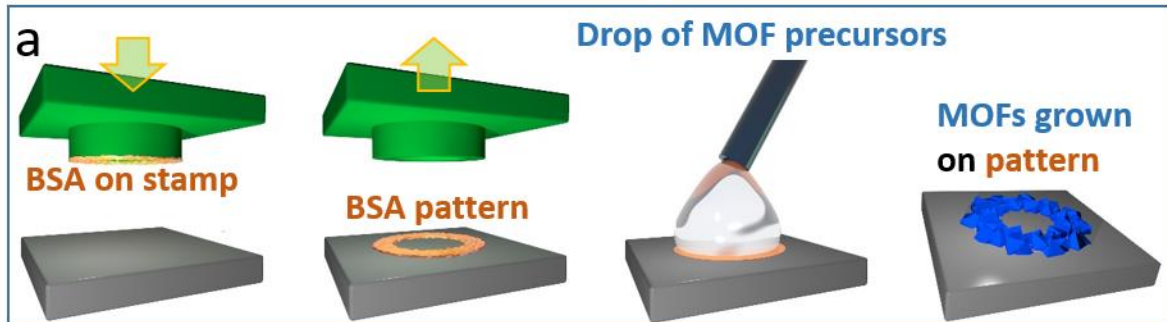
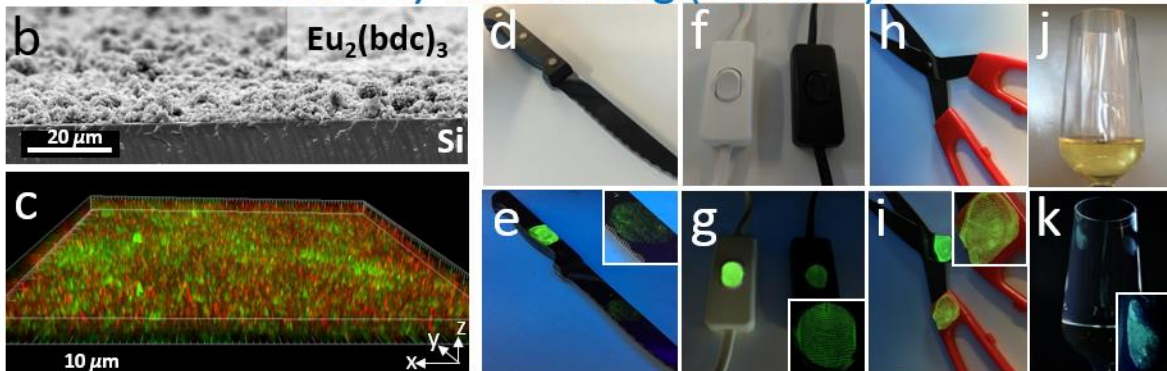


Figure 3. (a) Schematic showing the formation of Enzyme@MOF capsules around an emulsion droplet containing a biomolecule; (b) ZIF-8 capsule prepared using the Pickering emulsion method (scale bar = 10 micron) and the hierarchical shell structure (inset);²⁹ (c) CLSM image of capsules in (b) loaded with FITC-tagged CalB; (d) MIL-88A capsules prepared using a microfluidic protocol;³⁰ (e) CLSM image of MIL-88A capsules in (d) loaded with fluorescein-labelled SiO₂; (f) size selective transesterification by CalB@ZIF-8 capsules (reaction products shown); (g) comparative synthesis yields of the DHA product in the glycerol oxidation by GDH@MIL-88A and free GDH; (h) changes in pH in the absence and presence of the inhibitor AChEI at pH 6 for AchE@MIL-88A (left) and free AchE (right). (Reproduced with permission

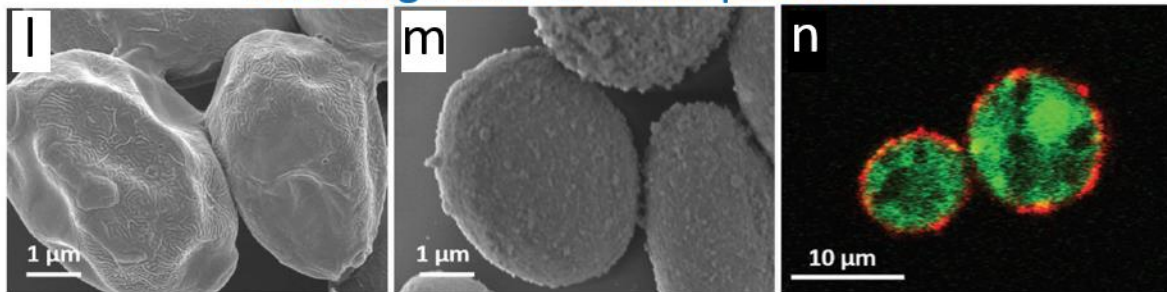
Positioning



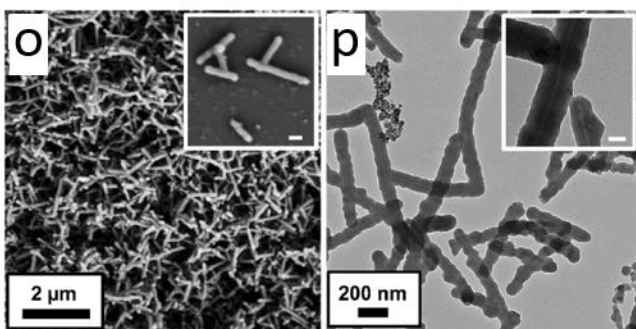
Delivery and Sensing (Forensic)



Biostorage and Cell manipulation



Biostorage, Virus manipulation



Biostorage, Biosensing

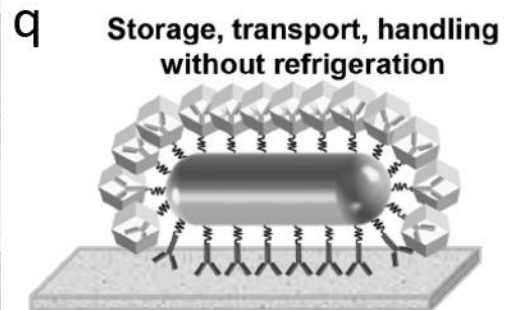


Figure 5. (a) Biomimetic replication of MOFs using a protein pattern, (b) perspective SEM images of $\text{Eu}_2(\text{bdc})_3$ thin films, (c) 3D view of super-resolution microscopy images of $\text{Eu}_2(\text{bdc})_3$ thin films (red) on BSA (green), and (d-k) photographs of $\text{Tb}_2(\text{bdc})_3$ patterns grown from fingerprint residues on various objects in visible (d-j) and under UV light (e-k).³⁸ SEM images of native (l) and ZIF-8 coated (m) yeast cells; (n) cellular cross section image of ZIF-8 (red) coated yeast cells (green, cytoplasm).¹⁰ SEM (o) and TEM (p) of as-synthesized TMV@ZIF-8 structures.⁴¹ (q) Schematic illustrating the concept of using MOFs to enhance the thermal stability of antibody-based plasmonic biochips.⁴² (Reproduced with permission from the refs.: [10],[38],[41],[42]. Copyright 2015-2016 WILEY-VCH)

Table 1. Examples of *covalent grafting* of biomacromolecules on MOFs

MOF	Substrate	Linkage	Application	Ref.
$\text{NH}_2\text{-MIL88B}(\text{Cr})$	Trypsin	DCC	Proteomics	12
HKUST-1	Streptavidin	EDC/NHS	Sensing	13
$\text{NH}_2\text{-MIL53}(\text{Al})$	β -Glucosidase	Glutaraldehyd	Biocatalysis	17
$\text{NH}_2\text{-UiO66}(\text{Zr})$	SEH	e	Biocatalysis	18
		Glutaraldehyd		
		e		

Table 2. Examples of *adsorption* of biomacromolecules on MOFs

MOF	Substrate(s)	Application	Ref.
ZIF-7, ZIF-67, ZIF-68, ZIF-70	GDH	Sensing	44
CYCU-4	Trypsin-FITC	Biocatalysis	19
H ₂ dtoaCu	DNA	DNA detection	48
Fe ₃ O ₄ @MIL100(Fe)	BSA	Separation	49
CYCU-4, UiO66(Zr)	Trypsin-NBD	Biocatalysis	20
LaMOF-GO	Hemoglobin, BSA	Sensing	50
MIL101(Cr)	DNA	DNA detection	43
NH ₂ -UiO68(Zr)	siRNA	Drug delivery	45
UiO66(Zr), NH ₂ -UiO66(Zr), MIL53(Al)	PPL	Biocatalysis	21
IRMOF-3	Primary antibody	Sensing	51
ZIF-8 on monoliths	Trypsin	Immobilization	52

Table 3. Example of *infiltration* of biomacromolecules into MOFs

MOF host	Substrate(s) guest	Application	Ref.
Tb-mesoMOF	Cytochrome c, Myoglobin, MP-11	Biocatalysis	22–25
CuJAST-1	Diphenylalanine	Nanomachine	53
MOF-74 isorecticular analogues	Vitamin B ₁₂ , Myoglobin, GFP	-	26
	β-ADR 15-peptide	-	54
	Proteins	-	55

Fe ₃ O ₄ @MIL100(Fe)	Various phosphopeptides	Separation	56
PCN-332, PCN-333	HRP, cytc, MP-11	Biocatalysis	57
NU-1000, PCN-600, CYCU-3	Cutinase	-	46
NU-1003	OPAA	Detoxificatio	27
PCN-128y		n	28
		Detoxificatio	
		n	
PCN-888	GOx and HRP	Biocatalysis	58
HKUST-1	Lipase from <i>B. subtilis</i>	Biocatalysis	59
PCN-333	MP-11	Sensing	60

Table 4. Example of *one-pot embedding* of biomacromolecules within MOFs.

MOF	Biomacromolecule(s)	Application	Ref.
ZIF-8	BSA, FITC-BSA, HSA, OVA, DQ-OVA, Insulin, Hemoglobin, Lysozyme, Ribonuclease A, (PQQ)GDH, Lipase, HRP, Trypsin, Urease	Bio-banking, bioprocessing, delivery	8,38
ZIF-8	DNA	Bio-banking	
HKUST-1	BSA	Bio-banking	

MIL-88A(Fe)	BSA	Bio-banking		32
Eu-/Tb-BDC	BSA	Bio-banking and sensing		
ZIF-90	Catalase, FITC-catalase	Bioprocessing		33
ZIF-8	Cytc, HRP, Lipase	Bioprocessing		
ZIF-10	Cytc	Bioprocessing		
ZIF-8	OVA, FITC-OVA	Delivery		37

AUTHOR INFORMATION

Corresponding Authors

* christian.doonan@adelaide.edu.au; d.bradshaw@soton.ac.uk; paolo.falcaro@tugraz.at.

Author Contributions

The manuscript was written through contributions of all authors. All authors have given approval to the final version of the manuscript.

Biographical Information

Christian Doonan is a chemist working as a professor and Director of the Centre for Advanced Nanomaterials at the University of Adelaide (Australia).

Raffaele Ricco is an organic chemist working as assistant professor at Graz University of Technology (Austria).

Kang Liang is a materials scientist working as a research fellow at the University of New South Wales (Australia).

Dr Darren Bradshaw is an Associate Professor at the University of Southampton, UK, where he leads the Functional Inorganic, Materials and Supramolecular chemistry research section.

Paolo Falcaro is a materials scientists working as a professor at Graz University of Technology (Austria) and as adjunct professor at the University of Adelaide (Australia).

ACKNOWLEDGMENT

RR acknowledges the TU Graz Research and Technology House.

ABBREVIATIONS

Bio(macro)molecules:

BSA=bovine serum albumin; HAS=human serum albumin; HRP=horseradish peroxidase; MP-11=microperoxidase; ADR=adrenoreceptor; GFP=green fluorescent protein; OPAA=organophosphorus acid anhydrolase; GOx=glucose oxidase; HRP=horseradish peroxidase; CalB=Candida Antarctica lipase B; cytc=Cytochrome c; siRNA=small interfering RNA; NBD=4-Nitro-2,1,3-benzoxadiazole; (PQQ)GDH=glucose dehydrogenase (pyrroloquinoline-quinone-dependent); AChE=acetylcholinesterase; PPL=porcine pancreatic lipase; SEH=Soybean Epoxide Hydrolase; FITC=fluorescein isothiocyanate; NHS=N-hydroxysuccinimide; DCC=dicyclohexylcarbodiimide; EDC=1-Ethyl-3-(3-dimethylaminopropyl)carbodiimide; PVP=polyvinylpyrrolidone; Glu=glutamic acid; Asp=aspartic acid; PDA=polydopamine; SAXS=Small Angle X-ray Scattering.

MOF acronyms and their full formulas (H₂O omitted):

HKUST-1	Cu ₃ (BTC) ₂ , BTC ³⁻ =benzene-1,3,5-tricarboxylate (trimesate)
IRMOF-3	Zn ₄ O(NH ₂ BDC) ₃ , NH ₂ BDC ²⁻ =2-aminoterephthalate
MOF-74	M ₂ O ₂ (DOT or L) ₂ , M=Mg, Zn, Co, Ni, DOT ²⁻ =2,5-dihydroxyterephthalate
MIL53(Al)	Al(OH)(BDC), BDC ²⁻ =benzene-1,4-dicarboxylate (terephthalate)

MIL88B(Cr)	$\text{Cr}_3\text{O}(\text{fum})_3$, fum^{2-} =fumarate
MIL100(Fe)	$\text{Fe}_3\text{OX}(\text{BTC})_2$, X=F, Cl, OH
MIL101(Cr)	$\text{Cr}_3\text{O}(\text{OH})(\text{BDC})_3$
ZIF-8	$\text{Zn}(\text{mIm})_2$; mIm^- =2-methylimidazolate
UiO66(Zr)	$\text{Zr}_6\text{O}_4(\text{OH})_4(\text{BDC})_6$
UiO68(Zr)	$\text{Zr}_6\text{O}_4(\text{OH})_4(\text{aTPDC})_6$, aTPDC^{2-} =2'-amino- <i>p</i> -terphenyl-4,4''-dicarboxylate
CYCU-3/4	$\text{Al}(\text{OH})(\text{SDC})$, SDC^{2-} =4,4'-stilbenedicarboxylate, with MIL-68 (CYCU-3) or MIL-53 (CYCU-4) structure
PCN-128y	$\text{Zr}_6\text{O}_4(\text{OH})_4(\text{ETTC})_3$, ETTC^{4-} =4 ¹ ,4 ³ ,4 ⁵ ,4 ⁷ -(ethene-1,1,2,2-tetrayl)tetrakis-([1,1'-biphenyl]-4-carboxylate
PCN-332	$\text{M}_3\text{O}(\text{BTTC})_4$, M=Fe, Al, V, Sc, In, BTTC^{3-} = benzo-(1,2;3,4;5,6)-tris(thiophene-2'-carboxylate)
PCN-333	$\text{M}_3\text{O}(\text{TATB})_4$, M=Fe, Al, V, Sc, In, TATB^{3-} = 4,4',4''-[1,3,5]Triazine-2,4,6-triyl-tris-benzoate
PCN-600	$\text{Fe}_3\text{O}(\text{TCPP})_3$, TCPP^{4-} =4,4',4'',4'''-(Porphine-5,10,15,20-tetrayl)tetrakisbenzoate
PCN-888	$\text{Al}_3\text{O}(\text{OH})(\text{HTB})_2$, HTB^{3-} =4,4',4''-(1,3,3a1,4,6,7,9-Heptaazaphenalene-2,5,8-triyl)tribenzoate
NU-1000	$\text{Zr}_6\text{O}_4(\text{OH})_4(\text{TBAPy})_3$, TBAPy^{4-} =Pyrene-1,3,6,8-tetrakisbenzoate
NU-1003	$\text{Zr}_6\text{O}_4(\text{OH})_4(\text{L1})_3$, L1^{4-} =Pyrene-1,3,6,8-tetrakis-2-(6-naphthoate)
Tb-mesoMOF	$\text{Tb}(\text{TATB})$
LaMOF	$\text{La}(\text{BTC})$

H ₂ dtoaCu	Cu(dtoa), dtoa ²⁻ =dithiooxamide anion
CuJAST-1	Cu ₂ (BDC) ₂ (dabco), dabco=1,4-Diazabicyclo[2.2.2]octane

REFERENCES

- (1) Yaghi, O. M.; O’Keeffe, M.; Ockwig, N. W.; Chae, H. K.; Eddaoudi, M.; Kim, J. Reticular Synthesis and the Design of New Materials. *Nature* **2003**, *423*, 705–714.
- (2) Falcaro, P.; Ricco, R.; Yazdi, A.; Imaz, I.; Furukawa, S.; Maspoth, D.; Ameloot, R.; Evans, J. D.; Doonan, C. J. Application of Metal and Metal Oxide nanoparticles@MOFs. *Coord. Chem. Rev.* **2016**, *307*, 237–254.
- (3) Falcaro, P.; Ricco, R.; Doherty, C. M.; Liang, K.; Hill, A. J.; Styles, M. J. MOF Positioning Technology and Device Fabrication. *Chem. Soc. Rev.* **2014**, *43*, 5513–60.
- (4) Furukawa, H.; Cordova, K. E.; O’Keeffe, M.; Yaghi, O. M. The Chemistry and Applications of Metal-Organic Frameworks. *Science* **2013**, *341*, 1230444.
- (5) Wilmer, C. E.; Leaf, M.; Lee, C. Y.; Farha, O. K.; Hauser, B. G.; Hupp, J. T.; Snurr, R. Q. Large-Scale Screening of Hypothetical Metal–organic Frameworks. *Nat. Chem.* **2011**, *4*, 83–89.
- (6) Horcajada, P.; Gref, R.; Baati, T.; Allan, P. K.; Maurin, G.; Couvreur, P.; Férey, G.; Morris, R. E.; Serre, C. Metal–Organic Frameworks in Biomedicine. *Chem. Rev.* **2012**, *112*, 1232–1268.
- (7) Giménez-Marqués, M.; Hidalgo, T.; Serre, C.; Horcajada, P. Nanostructured Metal–organic Frameworks and Their Bio-Related Applications. *Coord. Chem. Rev.* **2016**, *307*, 342–360.
- (8) Liang, K.; Ricco, R.; Doherty, C. M.; Styles, M. J.; Bell, S.; Kirby, N.; Mudie, S.; Haylock, D.; Hill, A. J.; Doonan, C. J.; Falcaro, P. Biomimetic Mineralization of Metal–Organic Frameworks as Protective Coatings for Biomacromolecules. *Nat. Commun.* **2015**, *6*, 7240.
- (9) Garai, A.; Shepherd, W.; Huo, J.; Bradshaw, D. Biomineral-Inspired Growth of Metal–organic Frameworks in Gelatin Hydrogel Matrices. *J. Mater. Chem. B* **2013**, *1*, 3678–3684.
- (10) Liang, K.; Richardson, J. J.; Cui, J.; Caruso, F.; Doonan, C. J.; Falcaro, P. Metal–Organic Framework Coatings as Cytoprotective Exoskeletons for Living Cells. *Adv. Mater.* **2016**, *28*, 7910–7914.
- (11) Ricco, R.; Pfeiffer, C.; Sumida, K.; Sumby, C. J.; Falcaro, P.; Furukawa, S.; Champness, N. R.; Doonan, C. J. Emerging Applications of Metal–organic Frameworks. *CrystEngComm* **2016**, *18*, 6532–6542.
- (12) Shih, Y.-H.; Lo, S.-H.; Yang, N.-S.; Singco, B.; Cheng, Y.-J.; Wu, C.-Y.; Chang, I.-H.; Huang, H.-Y.; Lin, C.-H. Trypsin-Immobilized Metal–Organic Framework as a Biocatalyst In Proteomics Analysis. *ChemPlusChem* **2012**, *77*, 982–986.
- (13) Ling, P.; Lei, J.; Zhang, L.; Ju, H. Porphyrin-Encapsulated Metal–Organic Frameworks as Mimetic Catalysts for Electrochemical DNA Sensing via Allosteric Switch of Hairpin DNA. *Anal. Chem.* **2015**, *87*, 3957–3963.

- (14) Jung, S.; Park, S. Dual-Surface Functionalization of Metal-Organic Frameworks for Enhancing the Catalytic Activity of *Candida Antarctica* Lipase B in Polar Organic Media. *ACS Catal.* **2016**, 438–442.
- (15) Nakajima, N.; Ikada, Y. Mechanism of Amide Formation by Carbodiimide for Bioconjugation in Aqueous Media. *Bioconjug. Chem.* **1995**, 6, 123–130.
- (16) Avrameas, S. Coupling of Enzymes to Proteins with Glutaraldehyde. *Immunochemistry* **1969**, 6, 43–52.
- (17) Doherty, C. M.; Greci, G.; Riccò, R.; Mardel, J. I.; Reboul, J.; Furukawa, S.; Kitagawa, S.; Hill, A. J.; Falcaro, P. Combining UV Lithography and an Imprinting Technique for Patterning Metal-Organic Frameworks. *Adv. Mater.* **2013**, 25, 4701–4705.
- (18) Cao, S.-L.; Yue, D.-M.; Li, X.-H.; Smith, T. J.; Li, N.; Zong, M.-H.; Wu, H.; Ma, Y.-Z.; Lou, W.-Y. Novel Nano-/Micro-Biocatalyst: Soybean Epoxide Hydrolase Immobilized on UiO-66-NH₂ MOF for Efficient Biosynthesis of Enantiopure (*R*)-1, 2-Octanediol in Deep Eutectic Solvents. *ACS Sustain. Chem. Eng.* **2016**, 4, 3586–3595.
- (19) Liu, W.-L.; Lo, S.-H.; Singco, B.; Yang, C.-C.; Huang, H.-Y.; Lin, C.-H. Novel trypsin-FITC@MOF Bioreactor Efficiently Catalyzes Protein Digestion. *J. Mater. Chem. B* **2013**, 1, 928–932.
- (20) Liu, W.-L.; Wu, C.-Y.; Chen, C.-Y.; Singco, B.; Lin, C.-H.; Huang, H.-Y. Fast Multipoint Immobilized MOF Bioreactor. *Chem. – Eur. J.* **2014**, 20, 8923–8928.
- (21) Liu, W.-L.; Yang, N.-S.; Chen, Y.-T.; Lirio, S.; Wu, C.-Y.; Lin, C.-H.; Huang, H.-Y. Lipase-Supported Metal-Organic Framework Bioreactor Catalyzes Warfarin Synthesis. *Chem. - Eur. J.* **2015**, 21, 115–119.
- (22) Chen, Y.; Lykourinou, V.; Vetromile, C.; Hoang, T.; Ming, L.-J.; Larsen, R. W.; Ma, S. How Can Proteins Enter the Interior of a MOF? Investigation of Cytochrome c Translocation into a MOF Consisting of Mesoporous Cages with Microporous Windows. *J. Am. Chem. Soc.* **2012**, 134, 13188–13191.
- (23) Chen, Y.; Lykourinou, V.; Hoang, T.; Ming, L.-J.; Ma, S. Size-Selective Biocatalysis of Myoglobin Immobilized into a Mesoporous Metal–Organic Framework with Hierarchical Pore Sizes. *Inorg. Chem.* **2012**, 51, 9156–9158.
- (24) Lykourinou, V.; Chen, Y.; Wang, X.-S.; Meng, L.; Hoang, T.; Ming, L.-J.; Musselman, R. L.; Ma, S. Immobilization of MP-11 into a Mesoporous Metal–Organic Framework, MP-11@mesoMOF: A New Platform for Enzymatic Catalysis. *J. Am. Chem. Soc.* **2011**, 133, 10382–10385.
- (25) Chen, Y.; Han, S.; Li, X.; Zhang, Z.; Ma, S. Why Does Enzyme Not Leach from Metal–Organic Frameworks (MOFs)? Unveiling the Interactions between an Enzyme Molecule and a MOF. *Inorg. Chem.* **2014**, 53, 10006–10008.
- (26) Deng, H.; Grunder, S.; Cordova, K. E.; Valente, C.; Furukawa, H.; Hmadeh, M.; Gándara, F.; Whalley, A. C.; Liu, Z.; Asahina, S.; Kazumori, H.; O’Keeffe, M.; Terasaki, O.; Stoddart, J. F.; Yaghi, O. M. Large-Pore Apertures in a Series of Metal-Organic Frameworks. *Science* **2012**, 336, 1018–23.
- (27) Li, P.; Moon, S.-Y.; Guelta, M. A.; Lin, L.; Gómez-Gualdrón, D. A.; Snurr, R. Q.; Harvey, S. P.; Hupp, J. T.; Farha, O. K. Nanosizing a Metal–Organic Framework Enzyme Carrier for Accelerating Nerve Agent Hydrolysis. *ACS Nano* **2016**, 10, 9174–9182.
- (28) Li, P.; Moon, S.-Y.; Guelta, M. A.; Harvey, S. P.; Hupp, J. T.; Farha, O. K. Encapsulation of a Nerve Agent Detoxifying Enzyme by a Mesoporous Zirconium Metal–Organic

- Framework Engenders Thermal and Long-Term Stability. *J. Am. Chem. Soc.* **2016**, *138*, 8052–8055.
- (29) Huo, J.; Aguilera-Sigalat, J.; El-Hankari, S.; Bradshaw, D. Magnetic MOF Microreactors for Recyclable Size-Selective Biocatalysis. *Chem Sci* **2015**, *6*, 1938–1943.
 - (30) Jeong, G.-Y.; Ricco, R.; Liang, K.; Ludwig, J.; Kim, J.-O.; Falcaro, P.; Kim, D.-P. Bioactive MIL-88A Framework Hollow Spheres via Interfacial Reaction In-Droplet Microfluidics for Enzyme and Nanoparticle Encapsulation. *Chem. Mater.* **2015**, *27*, 7903–7909.
 - (31) Wang, Y.; Hou, C.; Zhang, Y.; He, F.; Liu, M.; Li, X. Preparation of Graphene Nano-Sheet Bonded PDA/MOF Microcapsules with Immobilized Glucose Oxidase as a Mimetic Multi-Enzyme System for Electrochemical Sensing of Glucose. *J Mater Chem B* **2016**, *4*, 3695–3702.
 - (32) Shieh, F.-K.; Wang, S.-C.; Yen, C.-I.; Wu, C.-C.; Dutta, S.; Chou, L.-Y.; Morabito, J. V.; Hu, P.; Hsu, M.-H.; Wu, K. C.-W.; Tsung, C.-K. Imparting Functionality to Biocatalysts via Embedding Enzymes into Nanoporous Materials by a de Novo Approach: Size-Selective Sheltering of Catalase in Metal–Organic Framework Microcrystals. *J. Am. Chem. Soc.* **2015**, *137*, 4276–4279.
 - (33) Lyu, F.; Zhang, Y.; Zare, R. N.; Ge, J.; Liu, Z. One-Pot Synthesis of Protein-Embedded Metal–Organic Frameworks with Enhanced Biological Activities. *Nano Lett.* **2014**, *14*, 5761–5765.
 - (34) Lu, G.; Li, S.; Guo, Z.; Farha, O. K.; Hauser, B. G.; Qi, X.; Wang, Y.; Wang, X.; Han, S.; Liu, X.; DuChene, J. S.; Zhang, H.; Zhang, Q.; Chen, X.; Ma, J.; Loo, S. C. J.; Wei, W. D.; Yang, Y.; Hupp, J. T.; Huo, F. Imparting Functionality to a Metal–organic Framework Material by Controlled Nanoparticle Encapsulation. *Nat. Chem.* **2012**, *4*, 310–316.
 - (35) Gkaniatsou, E.; Sicard, C.; Ricoux, R.; Mahy, J.-P.; Steunou, N.; Serre, C. Metal–organic Frameworks: A Novel Host Platform for Enzymatic Catalysis and Detection. *Mater Horiz* **2017**, *4*, 55–63.
 - (36) He, H.; Han, H.; Shi, H.; Tian, Y.; Sun, F.; Song, Y.; Li, Q.; Zhu, G. Construction of Thermophilic Lipase-Embedded Metal–Organic Frameworks via Biomimetic Mineralization: A Biocatalyst for Ester Hydrolysis and Kinetic Resolution. *ACS Appl. Mater. Interfaces* **2016**, *8*, 24517–24524.
 - (37) Zhang, Y.; Wang, F.; Ju, E.; Liu, Z.; Chen, Z.; Ren, J.; Qu, X. Metal–Organic–Framework-Based Vaccine Platforms for Enhanced Systemic Immune and Memory Response. *Adv. Funct. Mater.* **2016**, *26*, 6454–6461.
 - (38) Liang, K.; Carbonell, C.; Styles, M. J.; Ricco, R.; Cui, J.; Richardson, J. J.; MasPOCH, D.; Caruso, F.; Falcaro, P. Biomimetic Replication of Microscopic Metal–Organic Framework Patterns Using Printed Protein Patterns. *Adv. Mater.* **2015**, *27*, 7293–7298.
 - (39) Carbonell, C.; Stylianou, K. C.; Hernando, J.; Evangelio, E.; Barnett, S. A.; Nettikadan, S.; Imaz, I.; MasPOCH, D. Femtolitre Chemistry Assisted by Microfluidic Pen Lithography. *Nat. Commun.* **2013**, *4*, 2173.
 - (40) Li, W.; Zhang, Y.; Xu, Z.; Meng, Q.; Fan, Z.; Ye, S.; Zhang, G. Assembly of MOF Microcapsules with Size-Selective Permeability on Cell Walls. *Angew. Chem. Int. Ed.* **2016**, *55*, 955–959.
 - (41) Li, S.; Dharmarwardana, M.; Welch, R. P.; Ren, Y.; Thompson, C. M.; Smaldone, R. A.; Gassensmith, J. J. Template-Directed Synthesis of Porous and Protective Core-Shell Bionanoparticles. *Angew. Chem. Int. Ed.* **2016**, *55*, 10691–10696.

- (42) Wang, C.; Tadepalli, S.; Luan, J.; Liu, K.-K.; Morrissey, J. J.; Kharasch, E. D.; Naik, R. R.; Singamaneni, S. Metal-Organic Framework as a Protective Coating for Biodiagnostic Chips. *Adv. Mater.* **2016**, 1604433.
- (43) Fang, J. M.; Leng, F.; Zhao, X. J.; Hu, X. L.; Li, Y. F. Metal-organic Framework MIL-101 as a Low Background Signal Platform for Label-Free DNA Detection. *The Analyst* **2014**, *139*, 801–806.
- (44) Ma, W.; Jiang, Q.; Yu, P.; Yang, L.; Mao, L. Zeolitic Imidazolate Framework-Based Electrochemical Biosensor for in Vivo Electrochemical Measurements. *Anal. Chem.* **2013**, *85*, 7550–7557.
- (45) He, C.; Lu, K.; Liu, D.; Lin, W. Nanoscale Metal-Organic Frameworks for the Co-Delivery of Cisplatin and Pooled siRNAs to Enhance Therapeutic Efficacy in Drug-Resistant Ovarian Cancer Cells. *J. Am. Chem. Soc.* **2014**, *136*, 5181–5184.
- (46) Li, P.; Modica, J. A.; Howarth, A. J.; Vargas L., E.; Moghadam, P. Z.; Snurr, R. Q.; Mrksich, M.; Hupp, J. T.; Farha, O. K. Toward Design Rules for Enzyme Immobilization in Hierarchical Mesoporous Metal-Organic Frameworks. *Chem* **2016**, *1*, 154–169.
- (47) Liang, K.; Coghlan, C. J.; Bell, S. G.; Doonan, C.; Falcato, P. Enzyme Encapsulation in Zeolitic Imidazolate Frameworks: A Comparison between Controlled Co-Precipitation and Biomimetic Mineralisation. *Chem. Commun.* **2015**, *52*, 473–476.
- (48) Ye, T.; Liu, Y.; Luo, M.; Xiang, X.; Ji, X.; Zhou, G.; He, Z. Metal-organic Framework-Based Molecular Beacons for Multiplexed DNA Detection by Synchronous Fluorescence Analysis. *The Analyst* **2014**, *139*, 1721.
- (49) Xiong, Z.; Ji, Y.; Fang, C.; Zhang, Q.; Zhang, L.; Ye, M.; Zhang, W.; Zou, H. Facile Preparation of Core-Shell Magnetic Metal-Organic Framework Nanospheres for the Selective Enrichment of Endogenous Peptides. *Chem. - Eur. J.* **2014**, *20*, 7389–7395.
- (50) Liu, J.-W.; Zhang, Y.; Chen, X.-W.; Wang, J.-H. Graphene Oxide-Rare Earth Metal-Organic Framework Composites for the Selective Isolation of Hemoglobin. *ACS Appl. Mater. Interfaces* **2014**, *6*, 10196–10204.
- (51) He, Y.; Wang, Y.; Yang, X.; Xie, S.; Yuan, R.; Chai, Y. Metal Organic Frameworks Combining CoFe₂O₄ Magnetic Nanoparticles as Highly Efficient SERS Sensing Platform for Ultrasensitive Detection of N-Terminal Pro-Brain Natriuretic Peptide. *ACS Appl. Mater. Interfaces* **2016**, *8*, 7683–7690.
- (52) Wen, L.; Gao, A.; Cao, Y.; Svec, F.; Tan, T.; Lv, Y. Layer-by-Layer Assembly of Metal-Organic Frameworks in Macroporous Polymer Monolith and Their Use for Enzyme Immobilization. *Macromol. Rapid Commun.* **2016**, *37*, 551–557.
- (53) Ikezoe, Y.; Washino, G.; Uemura, T.; Kitagawa, S.; Matsui, H. Autonomous Motors of a Metal-organic Framework Powered by Reorganization of Self-Assembled Peptides at Interfaces. *Nat. Mater.* **2012**, *11*, 1081–1085.
- (54) Hu, Z.; Jiang, J. A Helical Peptide Confined in Metal-Organic Frameworks: Microscopic Insight from Molecular Simulation. *Microporous Mesoporous Mater.* **2016**, *232*, 138–142.
- (55) Zhang, H.; Lv, Y.; Tan, T.; van der Spoel, D. Atomistic Simulation of Protein Encapsulation in Metal-Organic Frameworks. *J. Phys. Chem. B* **2016**, *120*, 477–484.
- (56) Chen, Y.; Xiong, Z.; Peng, L.; Gan, Y.; Zhao, Y.; Shen, J.; Qian, J.; Zhang, L.; Zhang, W. Facile Preparation of Core-Shell Magnetic Metal-Organic Framework Nanoparticles for the Selective Capture of Phosphopeptides. *ACS Appl. Mater. Interfaces* **2015**, *7*, 16338–16347.

- (57) Feng, D.; Liu, T.-F.; Su, J.; Bosch, M.; Wei, Z.; Wan, W.; Yuan, D.; Chen, Y.-P.; Wang, X.; Wang, K.; Lian, X.; Gu, Z.-Y.; Park, J.; Zou, X.; Zhou, H.-C. Stable Metal-Organic Frameworks Containing Single-Molecule Traps for Enzyme Encapsulation. *Nat. Commun.* **2015**, *6*, 5979.
- (58) Lian, X.; Chen, Y.-P.; Liu, T.-F.; Zhou, H.-C. Coupling Two Enzymes into a Tandem Nanoreactor Utilizing a Hierarchically Structured MOF. *Chem Sci* **2016**, *7*, 6969–6973.
- (59) Cao, Y.; Wu, Z.; Wang, T.; Xiao, Y.; Huo, Q.; Liu, Y. Immobilization of Bacillus Subtilis Lipase on a Cu-BTC Based Hierarchically Porous Metal–organic Framework Material: A Biocatalyst for Esterification. *Dalton Trans* **2016**, *45*, 6998–7003.
- (60) Gong, C.; Shen, Y.; Chen, J.; Song, Y.; Chen, S.; Song, Y.; Wang, L. Microperoxidase-11@PCN-333 (Al)/Three-Dimensional Macroporous Carbon Electrode for Sensing Hydrogen Peroxide. *Sens. Actuators B Chem.* **2017**, *239*, 890–897.